# Roughening transitions in parity-conserving growth processes

**Haye Hinrichsen**
*Max-Planck-Institut für Physik komplexer Systeme, Dresden*
**Géza Ódor**
*Res. Inst. for Techn. Phys. & Materials Sci. Budapest*

## Introduction

- Motivation: Surface growth $\leftrightarrow$ Non-eq. phase trans. to abs. states
- In equilibrium models roughening transition exists for $d \geq 2$ dimensions only. What is the situation in $d = 1$ ? Is that always rough with short ranged interaction? **NO !** In non-equilibrium models like: polynuclear growth process, roughening transition has been observed.
- We investigate discretized interface models: each site $i$ is associated with an integer height variable $h_i \in Z$. The following versions:

  Solid on solid (**SOS**) (a), Restricted solid-on-solid (**RSOS**)(b):

$$|h_i - h_j| \leq 1 \tag{1}$$

  with random sequential or parallel sub-lattice dynamics (c),(d).

- The order parameter we consider is the interface width:

$$W(N,t) = \left[\frac{1}{L}\sum_i h_i^2(t) - \left(\frac{1}{L}\sum_i h_i(t)\right)^2\right]^{1/2} \tag{2}$$

  In many cases systems exhibit simple Family-Vicsek (FV) scaling of the interface width:

$$W(N,t) \sim N^{\alpha} f(t/N^z) \tag{3}$$

  where $z = \alpha/\tilde{\beta}$, meaning initial *algebraic growth:* $W \sim t^{\tilde{\beta}}$ and after $\xi(t) > N$ a *saturation:* $W_{sat} \sim L^{\alpha}$. **In our case the roughening is not so simple.**

# Interface roughening universality

The FV scaling form of $W^2$ is invariant under $\Lambda$ (RG) rescaling:

$$x \to \Lambda x, \quad t \to \Lambda^z t, \quad h(x,t) \to \Lambda^{-\alpha} h(x,t)$$

The critical exponents $\tilde{\beta}$ and $z$ define **UNIVERSALITY CLASSES of interfaces** (determined by symmetry properties and associated with certain stochastic differential equations)

Examples:

- **E-W**: Transl. symm. in: $x$,$t$,$h$, $h \leftrightarrow -h$, $\{\tilde{\beta} = (\frac{1}{2} - \frac{d}{4}),\ z = 2\}$

$$\partial_t h(x,t) = v + \sigma \nabla^2 h(x,t) + \xi(x,t)$$

- **KPZ**: Galilean. symm., $h \not\leftrightarrow -h$, $\{\tilde{\beta} = \frac{1}{3},\ z = \frac{3}{2}\}$ (1d)

$$\partial_t h(x,t) = v + \sigma \nabla^2 h(x,t) + \lambda (\nabla h(x,t))^2 + \xi(x,t)$$

- **Self-similar**: $\{\tilde{\beta} = \frac{1}{2},\ z = 2\}$ (1d)
- **Random deposition** $\{\tilde{\beta} = \frac{1}{2},\ \alpha = \infty\}$ (1d)
- **Coupled-DP**: Observed in PNG, Fungal growths and Monomer adsorption-desorption (without hole digging) models:
  Translational symmetry in: $x$, but broken in $h$ (pinned)
  $\{\alpha = 0,\ \tilde{\beta} = 0,\ W(t) \sim \ln(t)^\gamma,\ W(L) \sim \ln(L)^\kappa,\ z = z_{DP} \simeq 1.58\}$

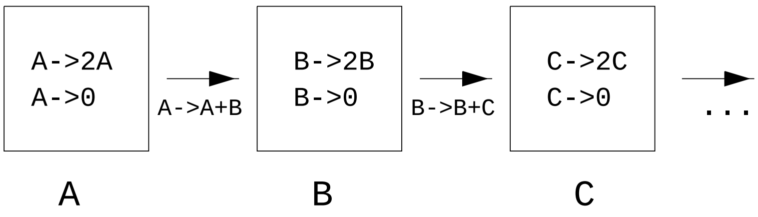

# Univ. classes of phase transitions to abs. states

## Directed Percolation (DP)

Wetting of a media, driven by a field (time direction). Reactions :

$$X \xrightarrow{k_1} 2X, \quad 2X \xrightarrow{k_2} X, \quad X \xrightarrow{k_3} \emptyset$$

Computer simulation of a 1-space + 1-time dimensional process at the percolation threshold ($k_1$, $k_3$, $k_3$ are tuned to criticality):

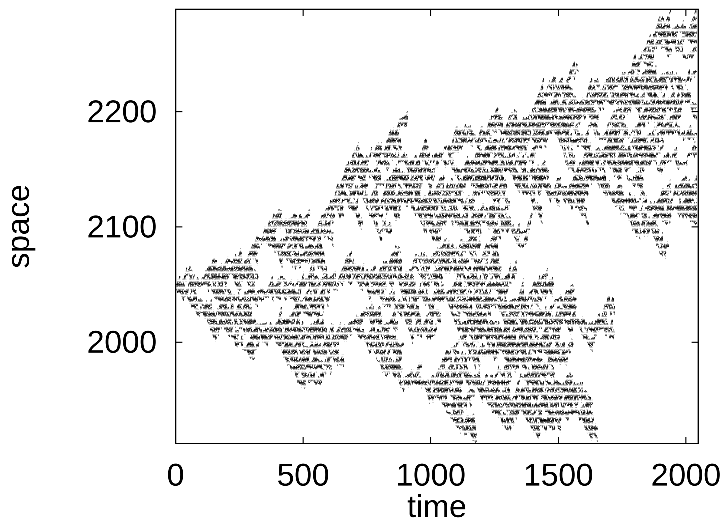


- forest fire
- epidemic without immunization
- auto-catalysis (contact-process) ...

Field theoretical description:

$$S[\psi, \phi] = \int d^d x \; dt \; \psi(\tau \partial_t \phi - D \nabla^2 \phi - \kappa)\phi + \frac{\Gamma}{2} \psi(\phi - \psi)\phi$$

Symmetry (time reversal + field exchange): $\phi(x, t) \leftrightarrow \psi(x, -t)$
.... $\rightarrow$ $\beta = \beta'$ $\rightarrow$ *hyperscaling law:* $4\delta + 2\eta = dz$

DP hypothesis (Janssen '81, Grassberger '82), No exact solution

## Univ. classes of phase transitions to abs. states

### Parity Conserving (PC) universality class

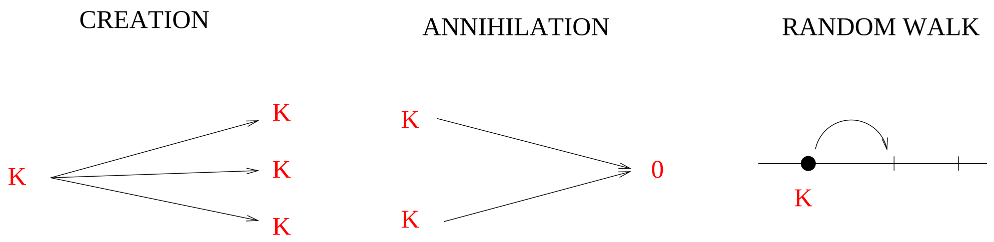


$$S[\psi,\phi]=\int d^dx\,dt\,\psi(\partial_t-D\nabla^2)\phi-\lambda(1-\psi^2)\phi^2+\sigma(1-\psi^2)\psi\phi$$

Symmetry (parity of fields):

$$\phi(x,t)\leftrightarrow-\phi(x,t)$$
$$\psi(x,t)\leftrightarrow-\psi(x,t)$$

Problem: *Two* critical dimensions: $d_c=2$, above which mean-field theory applies, and $d'_c\approx 4/3$, where for $d>d'_c$ ($d<d'_c$) the branching process is relevant (irrelevant) at the annihilation fixed point. (Cardy & Tauber '97).

... $\rightarrow$ The $d=1$ cannot be accessed by a controlled $\epsilon$-expansion.

**Some representatives of the PC universality class models :**

- Grassberger's A,B stochastic CA 1984
- BAWe, Takayasu et al '92, Jensen '94, Cardy & Tauber '96
- IMD, Park & Park '95
- NEKIM, Menyhárd '94, Menyhárd & Ódor '95, '96
- 3 species monomer-monomer model, Bassler & Browne '96
- GDK stochastic CA, Hinrichsen '97

# Definition of the dimer adsorption and desorption model

H. Hinrichsen and G. Ódor Phys. Rev. Lett **82** (1999) 1205.

A pair of neighboring sites $i$ and $j$ is selected at random. If the heights $h_i$ and $h_j$ are equal dimers are adsorbed with probability $p$

$$h_i \to h_i + 1 \qquad h_i \to h_j + 1 \tag{4}$$

or desorbed with probability $1-p$:

$$h_i \to h_i - 1 \qquad h_i \to h_j - 1 \qquad \text{if} \quad \min_{k \in <i,j>} h_k < h_i \tag{5}$$

where $k$ runs over the nearest neighbors of sites $i$ and $j$.

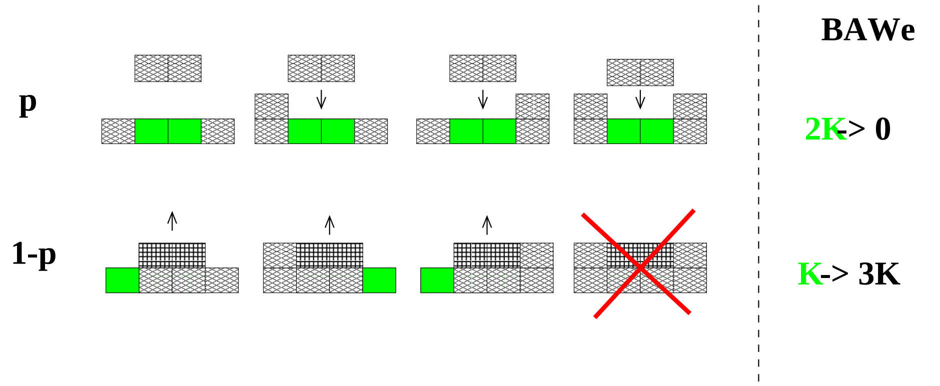


We investigated 1d RSOS, SOS random sequential (A,B) and parallel (sub-lattice) (C,D) versions.

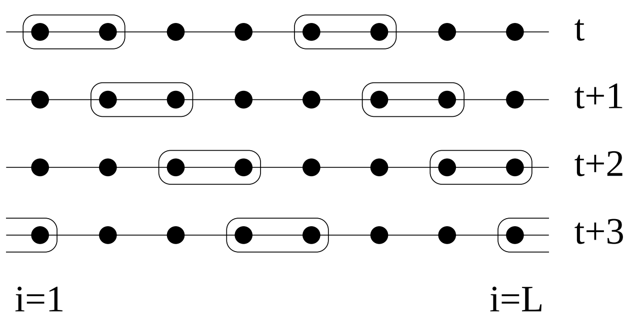


Figure 1: Variant C: Cyclic parallel updates on four different sub-lattices in a one spatial dimension.

## Phenomenology of the interface dynamics

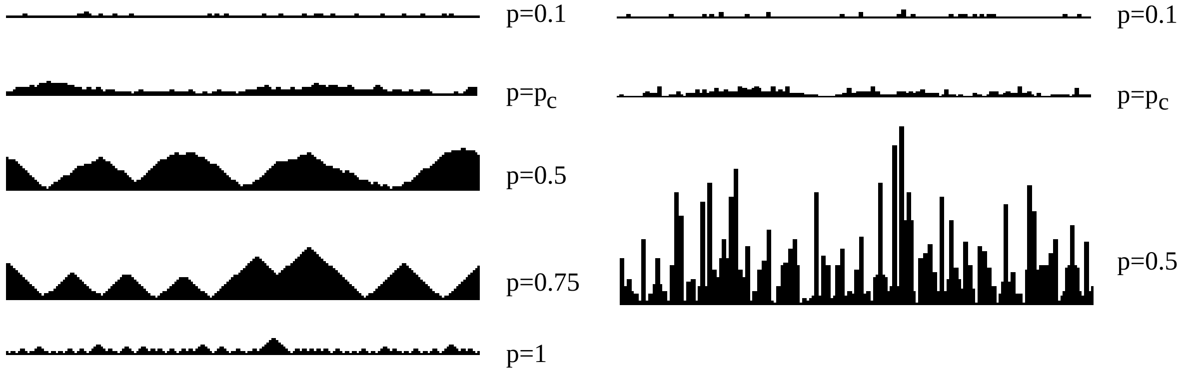


Figure 2: **RSOS** **SOS**

### Phase diagram of all versions

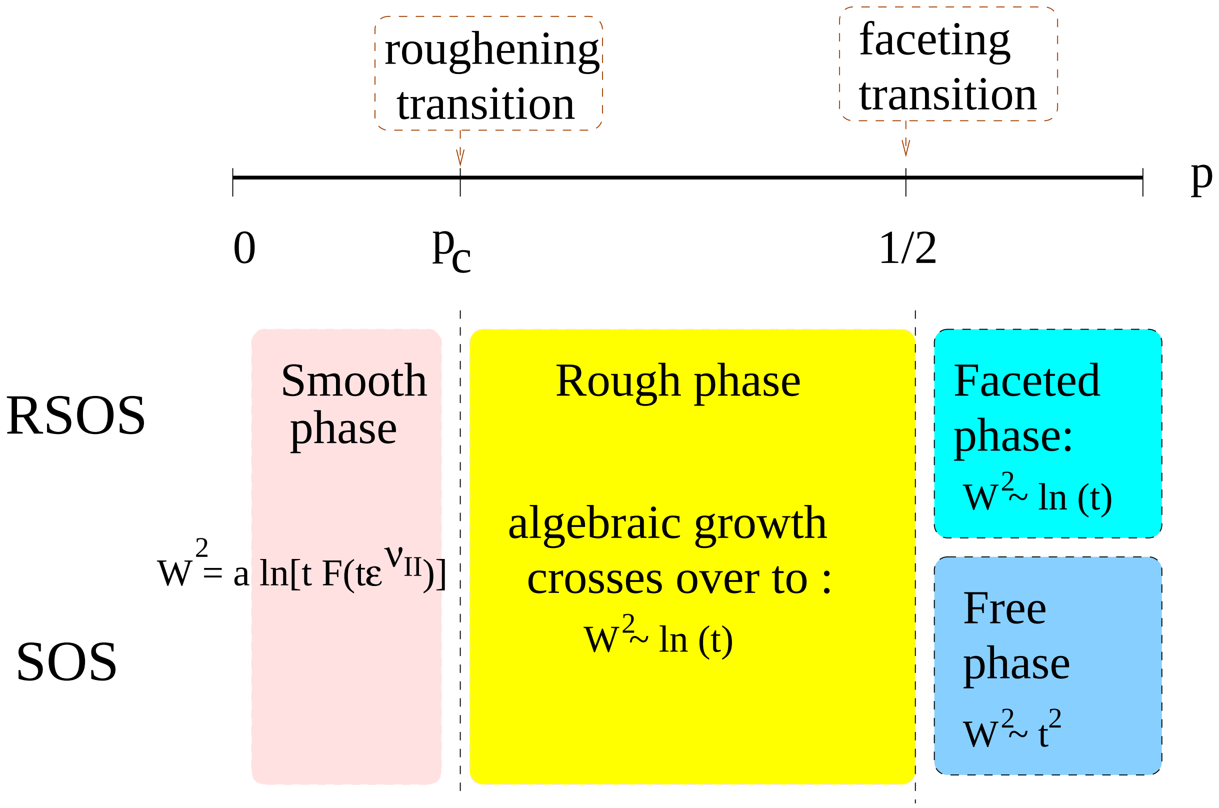


**The parallel and random sequential versions resulted in the same universal behavior!**

# Simulation results on the interface width

Monte-Carlo simulations starting from a flat interface $h_i(0) = 0$:

**The smooth phase $p < p_c$**

$$W^2(t, \epsilon) \simeq a \, \ln[t \, F(t\epsilon^{\nu_\parallel})] \,, \qquad (6)$$

where $a$ is an amplitude factor and $\epsilon = |p - p_c|$ denotes the distance from criticality. $F$ is a universal scaling function with the asymptotic behavior

$$F(\zeta) = \begin{cases} const & \text{if } \zeta \to 0 \\ \zeta^{-1} & \text{if } \zeta \to \infty \end{cases} \,. \qquad (7)$$

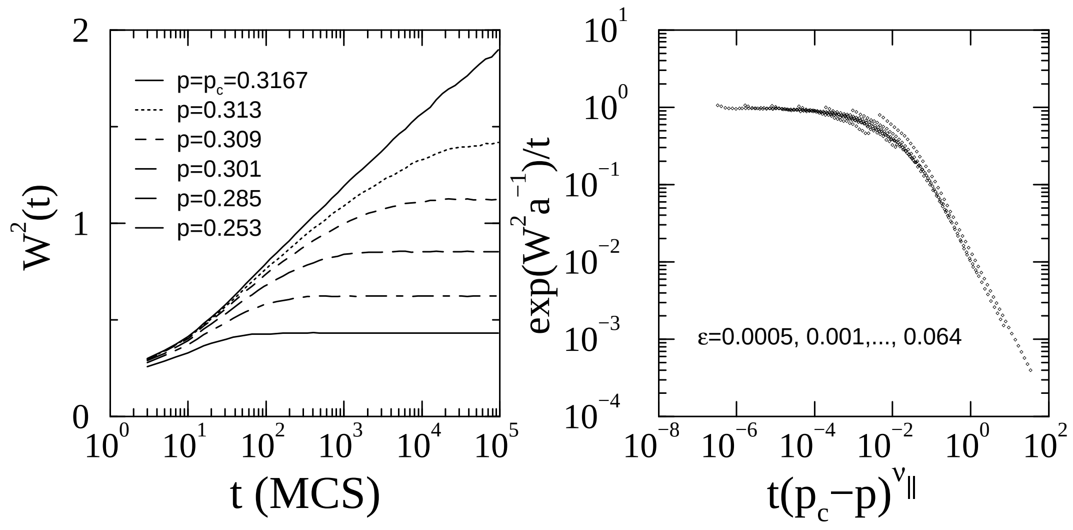


Figure 3: Left: The squared width $W^2(t)$ measured in variant A for various values of $p \leq p_c$. Right: Data collapse according to Eq. (6), visualizing the scaling function $F$.

# Simulation results on the interface width

## The roughening transition at $p = p_c$

*Logarithmic* growth similarly as in the monomer model.

$$W^2(L,t) \simeq a \ln[t\, G(t/L^z)]\,, \tag{8}$$

where $G$ is a universal scaling function with the same asymptotic behavior as in Eq. (7).

Plotting $\exp(W^2/a)/t$ against $t/L^z$ in the time interval $10 \leq t \leq 10^5$ for system sizes $L = 32, 64, \ldots, 4096$, we determine $a$ and $z$ by data collapse.

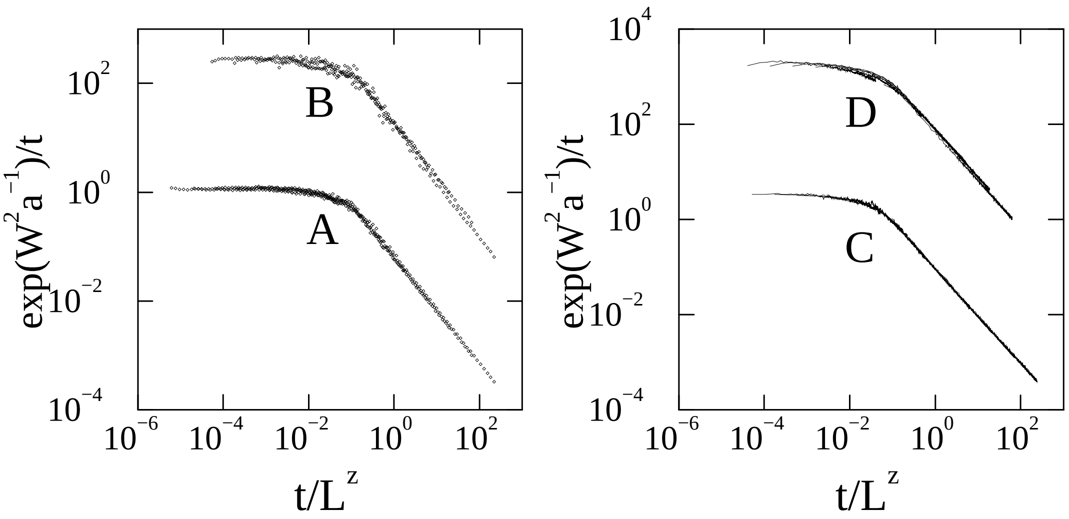


Figure 4: Finite-size scaling of the interface width $W(L,t)$ for variants A-D. The graphs show data collapses according to the scaling form (8), visualizing the scaling function $G$.

**The best data collapse is achieved with the dynamical exponent $z = 1.75$ in all cases corresponding to the PC universality class!** ($a$ is non-universal)

# Simulation results on the interface width

### The rough phase $p_c < p < 0.5$

The pinning centers prevents the interface from propagating. $\rightarrow$ Logarithmic asymptotic growth !

Pairwise annihilation of the pinning centers.

For small times: algebraic growth (the effect of the faceting transition), the crossover time diverges as $p \rightarrow 1/2$.

### The transition at $p = 0.5$

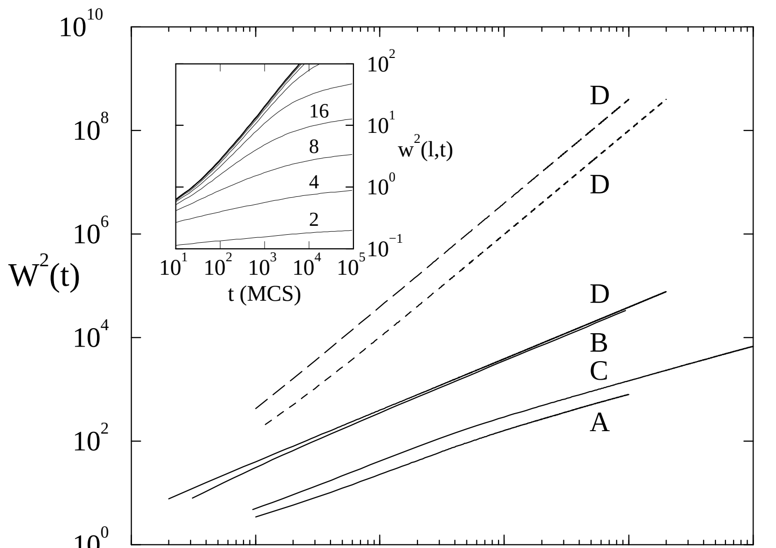


Figure 5: Power-law roughening of the width in large systems. The figure shows the squared width as a function of time at the transition $p = 0.5$ (solid lines), as well as above the transition for $p = 0.6$ (dashed line) and $p = 0.7$ (long-dashed line). The inset shows the squared local width of variant A for increasing box sizes $l = 2, 4, 8, 16, \ldots$ as a function of time.

# Simulation results on the interface width

**The transition at $p = 0.5$**

The width increases algebraically. We expect FV-scaling :

$$W(L,t) \sim L^{\tilde{\alpha}} f(t/L^{\tilde{\alpha}/\tilde{\beta}}) \,, \tag{9}$$

where $\tilde{\alpha}$ and $\tilde{\beta}$ are the roughening and the growth exponents, respectively. Finite size simulations reveal a more complex behavior.

## The RSOS case

Crossover following $t \simeq 5000$ MCS. For the long time behavior using finite size data collapse we find a roughening exponent $\tilde{\alpha} \simeq 1.2$ and a large dynamic exponent $\tilde{z} = \tilde{\alpha}/\tilde{\beta} \simeq 3$.

As inset shows the faceting transition displays **anomalous scaling** properties i.e., the *local* width $w(l,t)$ measured in boxes of sizes $l = 2, 4, 8, 16, \ldots$ does not saturate after a short time. Even for small box sizes it continues to increase over several time decades until it saturates due to the RSOS constraint.

## The SOS case

Purely diffusive mechanism. $W(t) \sim \sqrt{t}$. The columns are spatially decoupled, the width does not saturate in finite systems, i.e., the dynamic exponents $\tilde{\alpha}$ and $\tilde{z}$ have no physical meaning ($\alpha = \infty$ ?)

# Simulation results on the interface width

## The faceted/free rough phase for $p > 0.5$

### The RSOS case

Faceted configurations, the width first increases algebraically until the pinning centers become relevant and the system crosses over to a logarithmic increase of the width.

### The SOS case

Owing to the strong deposition rate and lack of height difference constraints the columns evolve "freely" as in random deposition processes:

$$W(t) \propto t$$

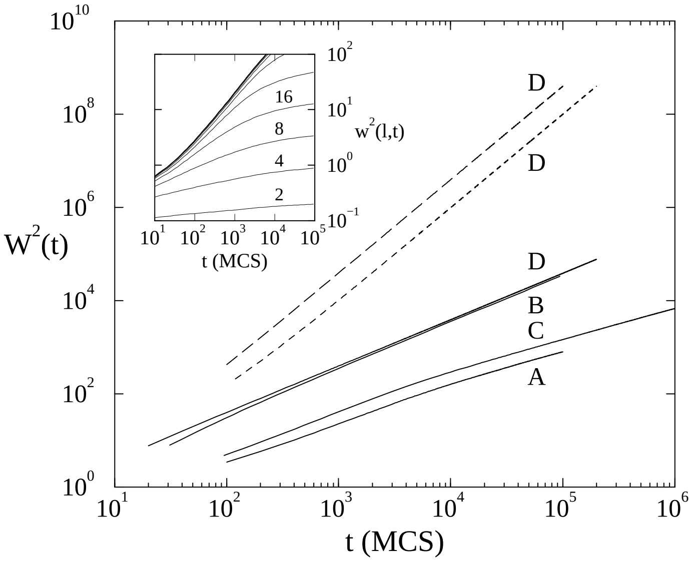


Figure 6: Power-law roughening of the width in large systems. The figure shows the squared width as a function of time at the transition $p = 0.5$ (solid lines), as well as above the transition for $p = 0.6$ (dashed line) and $p = 0.7$ (long-dashed line). The inset shows the squared local width of variant A for increasing box sizes $l = 2, 4, 8, 16, \ldots$ as a function of time.

# Critical properties of the first few layers

We expect **Parity conserving, BAWe** dynamics on the base level. Let us measure the density of sites at level $k$. Starting from a 'flat interface' we measure $n_0$, $n_1$ and $n_2$ at criticality. The densities are expected to decay as

$$n_k(t) \sim t^{-\delta_k}\,, \tag{10}$$

**We obtained PC class critical decay exponent for the base level:**

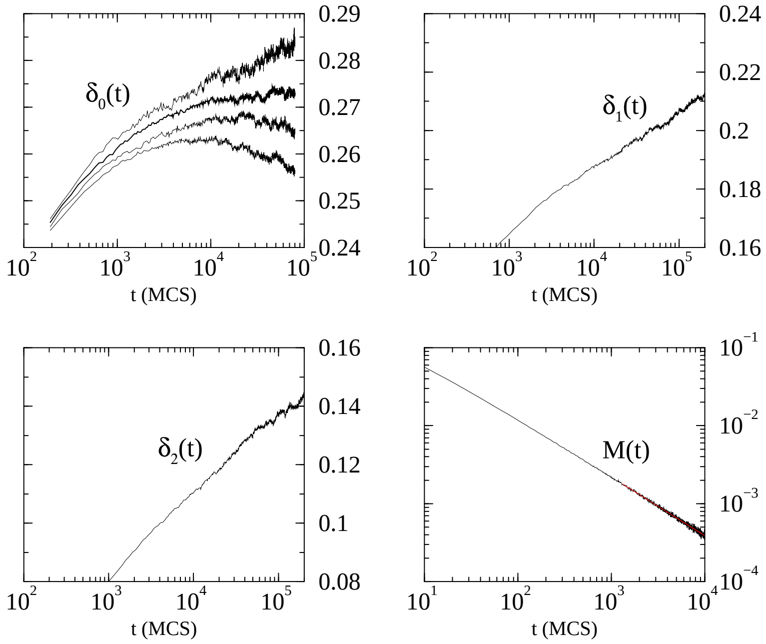


Figure 7: Effective exponents $\delta_k(t)$ measured in model C with 24000 sites averaged over $10^4$ samples. The first panel shows $\delta_0(t)$ with $p$ ranging from 0.3406 to 0.3409 from top to bottom, leading to the estimates $p_c = 0.3407(1)$ and $\delta_0 = 0.275(10)$. The curves for $\delta_1(t)$ and $\delta_2(t)$ at $p = p_c$ are shown in panel 2 and 3. The last panel shows the magnetization $M$ as a function of time.

$$M = \frac{1}{L}\sum_j (-1)^{h_j}\,, \tag{11}$$

$$|M| \sim t^{-\theta/\nu_{||}} \tag{12}$$

**The exponent $\theta$ – describing the spontaneous braking of translational invariance in height direction – is found to be universal ($\simeq 2.5$).** (Much larger than that of the monomer model)

# Finite size results on the base level at criticality

We checked the scaling form:

$$n_k(t, L, \epsilon) \sim t^{-\beta_k/\nu_\parallel} \, \Phi_k(t\, \epsilon^{\nu_\parallel}, \; t/L^z) \; . \tag{13}$$

by performing measurements of $n_0(t)$ for different system sizes.

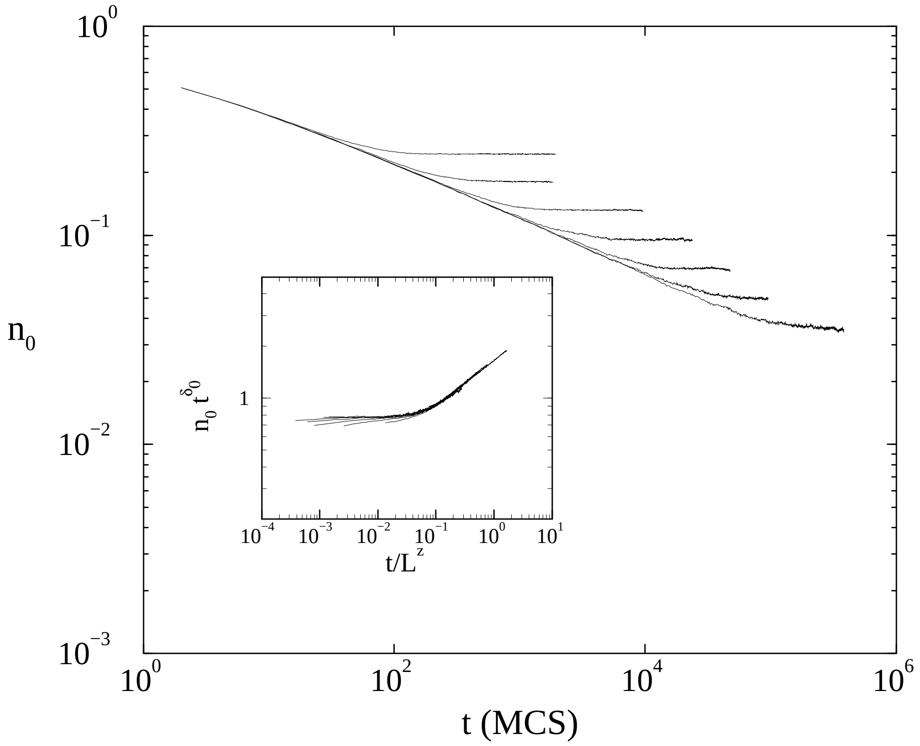


Figure 8: Finite size results for the parallel model for $L = 64, 128...4096$. The density at the bottom layer $n_0(t)$ is plotted as a function of time. The inset shows a data collapse which is explained in the text.

**The best data collapse is obtained for $\delta_0 \simeq 0.27$ and $z \simeq 1.7$, which is in agreement with the known PC exponents $\delta = 0.285(5)$, $z = 1.76(3)$.**

# Off-critical behavior

**The effect of back-coupling is: strong correction to scaling:**

By fitting the scaling form to the base level density:

$$n_0 \propto |p - p_c|^{\beta_0} \tag{14}$$

directly on the simulation data we have obtained a rough estimate $\beta_0 = 0.6(1)$ in variants A and C. This value **does not** agree with the expected PC university class value: $\beta_{PC} \approx 0.9$ !

More precise analyze of our simulation results is needed!

The local slopes of the log-log result data points $(i, i-1)$ have been determined by the form:

$$\beta_0(\epsilon_i) = \frac{\ln n_{0,i} - \ln n_{0,i-1}}{\ln \epsilon_i - \ln \epsilon_{i-1}} \quad , \tag{15}$$

where $\epsilon_i = p_c - p_i$, providing an estimate $\beta_0 = \lim_{\epsilon \to 0} \beta_0(\epsilon)$.

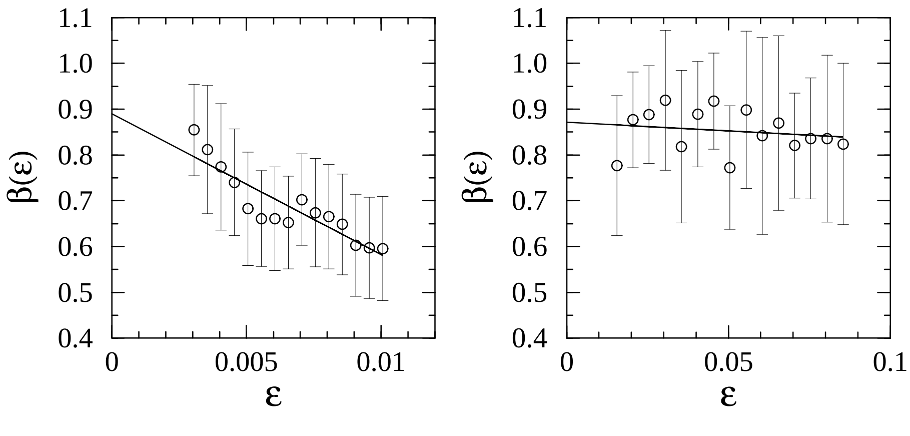


Figure 9: Left: The effective exponent $\beta_0(\epsilon)$ as a function of $\epsilon$ in model C with $L = 24000$ sites. After an equilibration of $4 \times 10^5$ time steps the bottom layer density is averaged over $10^3$ samples. A simple linear fit gives the estimate $\beta_0 \approx 0.89$. Right: Corresponding simulation results for the truncated model. Here the effective exponent is almost independent of $\epsilon$. Notice the different ranges of $\epsilon$.

# Summary of simulation results

| variant | A | B | C | D |
|---|---|---|---|---|
| restriction<br>updates | yes<br>random | no<br>random | yes<br>parallel | no<br>parallel |
| $p_c$ | 0.3167(2) | 0.292(1) | 0.3407(1) | 0.302(1) |
| $a$ | 0.172(5) | 0.23(1) | 0.162(4) | 0.19(1) |
| $z$ | 1.75(5) | 1.75(5) | 1.74(3) | 1.77(5) |
| $\beta_0$ | 0.89(10) | no result | 0.9(1) | no result |
| $\delta_0$ | 0.28(2) | 0.29(2) | 0.275(10) | 0.29(2) |
| $\delta_1$ | 0.22(2) | 0.21(2) | 0.205(15) | 0.21(2) |
| $\delta_2$ | 0.14(2) | 0.14(3) | 0.13(2) | 0.14(2) |
| $\theta/\nu_{\parallel}$ | 0.765(10) | 0.765(10) | 0.753(3) | no result |
| $\tilde{\alpha}$ | 1.2(1) | undefined | 1.25(5) | undefined |
| $\tilde{\beta}$ | 0.34(1) | 0.50(1) | 0.330(5) | 0.49(1) |

Table 1: Numerical estimates for the four variants of the dimer model at the roughening transition $p = p_c$ (upper part) and the transition $p = 0.5$ (lower part).

# Generic model: The unidirectionally coupled BAWe

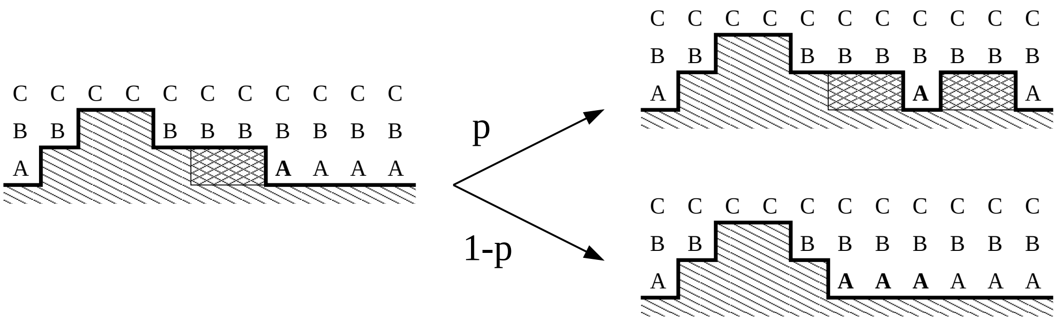


Figure 10: Extended particle interpretation. Dimers are adsorbed ($2A \rightarrow \emptyset$) and desorbed ($A \rightarrow 3A$) at the bottom layer. Similar processes take place at higher levels.

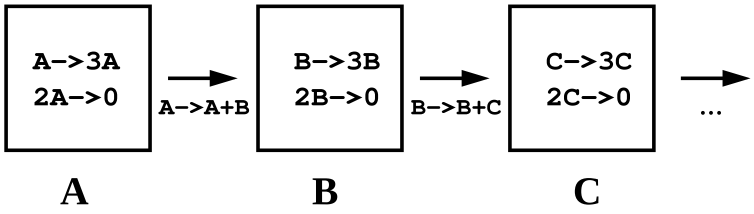


We investigate the dynamical scaling properties of the first few levels by simulation:

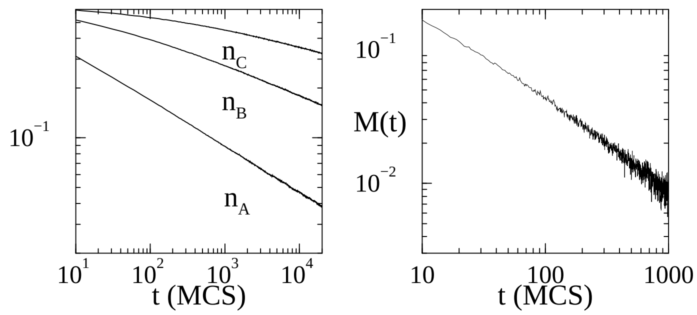


Figure 11: Unidirectionally coupled PC processes. Left: Densities $n_A, n_B, n_C$ as functions of time. Right: Magnetization $M(t)$ as a function of time averaged over 1000 independent realizations.

**We found PC class base level exponent ($\delta_A = 0.280(5)$) The effect of back-coupling is irrelevant ! Other exponents ($\delta_1,\ \delta_2,\ \theta$) are in agreement with that of the dimer model too.**

# Generic model: The unidirectionally coupled BAWe

## Mean-field approximation

$$\begin{aligned}\partial_t n_A &= \sigma n_A - \lambda n_A^2\,, \\ \partial_t n_B &= \sigma n_B - \lambda n_B^2 + \mu n_A\,, \\ \partial_t n_C &= \sigma n_C - \lambda n_C^2 + \mu n_B\,, \ \ldots\end{aligned} \tag{16}$$

where $\sigma$ and $\lambda$ are the rates for offspring production (dimer evaporation) and pair annihilation (dimer deposition), respectively, $\mu$ is an effective coupling constant between different particle species.

The mean-field critical point is $\sigma_c = 0$. For small values of $\sigma$ the stationary particle densities in the active state are given by

$$n_A = \frac{\sigma}{\lambda}, \;\; n_B \simeq \frac{\mu}{\lambda}\left(\frac{\sigma}{\mu}\right)^{1/2}, \;\; n_C \simeq \frac{\mu}{\lambda}\left(\frac{\sigma}{\mu}\right)^{1/4}, \tag{17}$$

corresponding to the mean field critical exponents

$$\beta_A^{MF} = 1, \quad \beta_B^{MF} = 1/2, \quad \beta_C^{MF} = 1/4, \ldots . \tag{18}$$

Valid at the critical dimension $d_c = 2$. Solving the asymptotic temporal behavior we find $\nu_{||} = 1$, implying that $\delta_k^{MF} = 2^{-k}$.

## Field theory:

$$\begin{aligned}&S[\psi_0, \psi_1, \psi_2, \ldots, \bar\psi_0, \bar\psi_1, \bar\psi_2, \ldots] = \\ &\int d^d x\, dt \sum_{k=0}^{\infty} \{\bar\psi_k(\partial_t - D\nabla^2)\psi_k - \lambda(1-\bar\psi_k^2)\psi_k^2 + \\ &\quad +\sigma(1-\bar\psi_k^2)\bar\psi_k\psi_k + \mu(1-\bar\psi_k)\bar\psi_{k-1}\psi_{k-1}\}\end{aligned} \tag{19}$$

where $\psi_{-1} = \bar\psi_{-1} \equiv 0$.

**Perturbative RG solution exhibits the same problem as found in one copy.** (Cardy & Tauber '96). **$\nu$ diverges under RG too!**

# Parity-conserving polynuclear growth models

We have invented the generalization of PNG model (Kertész, Wolf):

$$h_i(t+1) = \begin{cases} m(t)+1 & \text{with prob. } p \\ m(t) & \text{with prob. } 1-p \end{cases} , \tag{20}$$

where $m(t) = \max[h_{i-1}(t), h_i(t), h_{i+1}(t)]$.

For dimers it looks like:

If $h_i(t) \neq h_{i+1}(t)$, the heights are incremented by one step

$$\begin{aligned} h_i(t+1/2) &= h_i(t)+1 , \\ h_{i+1}(t+1/2) &= h_{i+1}(t)+1 . \end{aligned} \tag{21}$$

On the other hand, if the two heights are equal, they are are updated by the probabilistic rule

$$h_i(t+1/2) = h_{i+1}(t+1/2) \tag{22}$$

$$= \begin{cases} m(t)+1 & \text{with prob. } p \\ m(t) & \text{with prob. } 1-p \end{cases} , \tag{23}$$

where $m(t) = \max[h_{i-1}(t), h_i(t), h_{i+1}(t), h_{i+2}(t)]$.

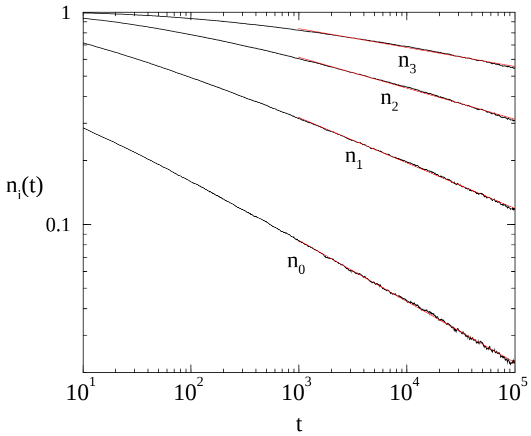


**We have obtained coupled-PC class scaling exponents**
$(\delta_0 = 0.28(1),\ \delta_1 = 0.21(2),\ \delta_2 = 0.14(2),\ \theta/\nu_{||} = 0.77)$
**in the co-moving frame !**

# Discussion

## Unusual scaling for random initial conditions

Starting from random initial conditions $h_i = 0, 1$ the densities $n_k$ turn out to decay much slower. For restricted variants we observe an algebraic decay of $n_0$ with an exponent $\delta_0 \simeq 0.13$ which differs significantly from the value 0.285 for flat initial conditions. Similarly, the critical properties of the faceting transition at $p = 0.5$ are affected by random initial conditions.

**Additional parity conservation law: Conservation the parity of the droplet size.** (There is no explicit random walk in the process).

For random initial condition only particles residing on the same sub-lattices can annihilate.

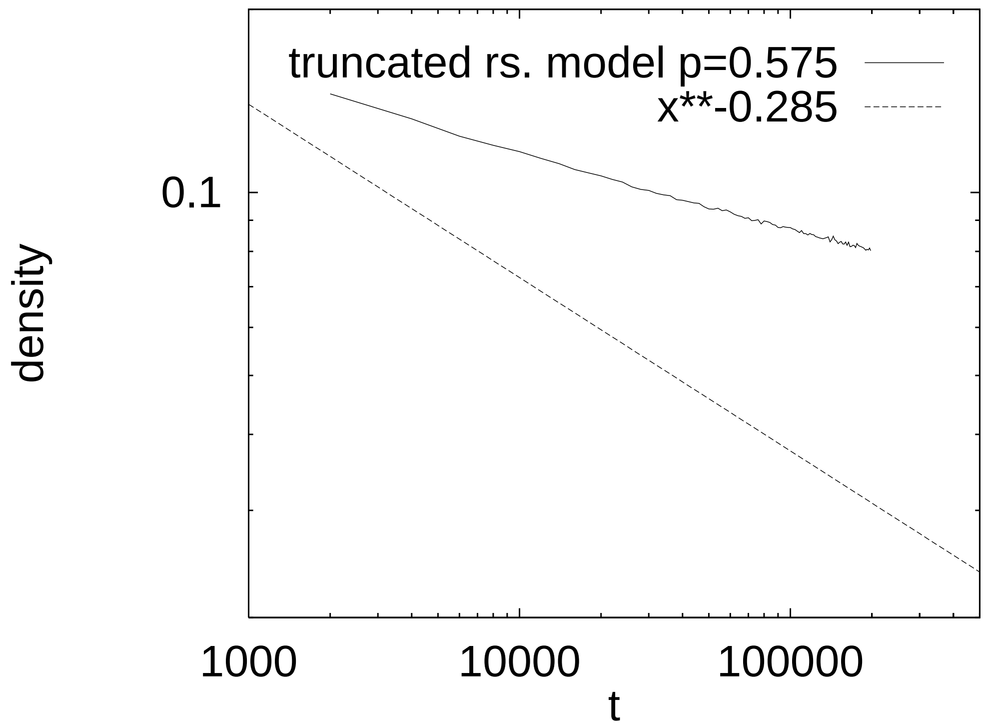


**Further investigation is under way ...**

# Comparison with other models

(a) Park & Khang ('98): Growth model with two symmetric particle species. Particles are adsorbed (desorbed) with probability $q$ $(1-q)$ except

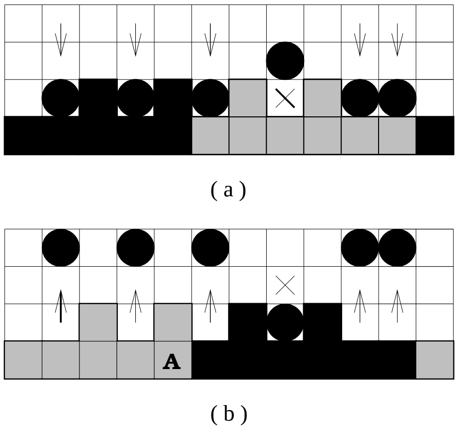


at those sites where the nearest neighbors are occupied by particles of the other (same) species. The dynamic rules mimic a PC transition with two symmetric absorbing states.

**Frozen lower layers → non-PC(DI) exponents (except mono-layer case)**

(b) Noh et. al ('98) Interacting monomer-dimer growth model:

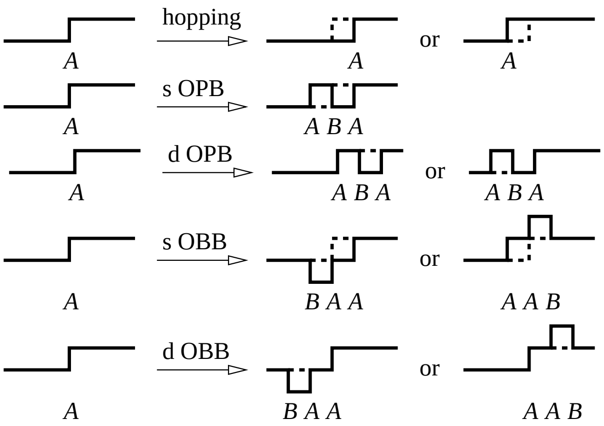


**Without OBB : mono-layers → PC class pre-roughening transition, with OBB : always rough surface**

# Conclusions

- A class of dimer adsorption-desorption models exhibiting roughening transition in 1d has been introduced
- The phase structure has been explored by simulations for four variants (RSOS, SOS with random-seq. or parallel sub-lattice updates). No difference in the universal properties between random-seq. and parallel sub-lattice versions has been detected.
- The roughening transition is universal and robust with respect to all dynamics used and belong to the same class as the unidirectional coupled BAWe.
- The effect of higher levels to the base level is non-relevant but causes strong correction to scaling.
- The interface growths logarithmically in the rough phase owing to the pinning centers.
- When the adsorption and desorption rates are equal, algebraic growth occurs with a faceting transition for RSOS models and a spiky "uncorrelated column, non-saturating" growth for the SOS case.
- In unrestricted cases, for strong dimer adsorption ($p > 0.5$) the pinning centers can not slow-down the surface growth and the interface roughness will grow linearly.
- A generalized PNG model with dimers has been invented and the same features are observed in the co-moving frame as in case of the RSOS parallel model.
- An extra symmetry has been observed causing unusual scaling for random initial conditions. Investigations are under way!